An Effective Approach to Computation of Forces in Viscous Incompressible Flows

B. Protas,*,† A. Styczek,* and A. Nowakowski*,‡

*Department of Aerodynamics, Institute of Aeronautics and Applied Mechanics, Warsaw University
of Technology, ul. Nowowiejska 24, 00-665 Warsaw, Poland; †Laboratoire de Physique et
Mécanique des Milieux Hétérogènes, C.N.R.S., U.R.A. 857, École Supérieure de
Physique et Chimie Industrielles, 10, rue Vauquelin, 75231 Paris Cedex 05,
France; and ‡Department of Chemical Engineering, UMIST,
P.O. Box 88, Manchester M60 1QD, United Kingdom
E-mail: bprotas@meil.pw.edu.pl

In the paper we present an effective method to compute forces in external flows of viscous incompressible fluids. It is an extension of the variational approach proposed initially by Quartapelle and Napolitano (1983, *AIAA J.* **21**, 911) and is particularly well adapted to the case where a vortex method is used to solve the hydrodynamic problem. The derived formula involves a harmonic function η and a convenient method for its determination is also shown. The effectiveness of the presented approach is confirmed by computational examples. © 2000 Academic Press

Key Words: hydrodynamic force; pressure; vortex methods.

1. INTRODUCTION

Determination of forces is crucial in many physical and engineering problems encountered in fluid dynamics. In the present paper we are interested in an approach which is particularly applicable when the fluid motion is determined using a vortex method. Below we will consider the external viscous flow past a single body whose shape may evolve in time. The flow domain will be denoted Ω and the boundary of the body $\partial\Omega$. In general we will thus have $\Omega = \Omega(t)$ and $\partial\Omega = \partial\Omega(t)$; in the following, however the symbol t will be dropped. We will restrict our attention to deformations which preserve the volume (the area in the plane case) of the obstacle and in which the impermeability condition is satisfied. The origin of the coordinate system will remain fixed at the obstacle. By definition, the force which is acting on the body can be expressed in the following way,

$$\mathbf{F} = \mathbf{F}^{\mathrm{P}} + \mathbf{F}^{\mu} = -\oint_{\partial\Omega} (-p\mathbf{n} + \bar{\bar{\Pi}}_{\mu} \cdot \mathbf{n})\, d\sigma, \tag{1}$$

231

where $\mathbf{F}^{\mathrm{P}}$ and $\mathbf{F}^{\mu}$ represent the contributions of pressure and viscous force, respectively, p is pressure, $\mathbf{n}$ is the unit normal (directed into the body) and $\bar{\bar{\Pi}}_{\mu}$ denotes the viscous stress tensor. For the incompressible Newtonian fluid it is given by

$$\bar{\bar{\Pi}}_{\mu} = \mu[\nabla\mathbf{V} + (\nabla\mathbf{V})^{\mathrm{T}}], \qquad (2)$$

with μ representing the viscosity of the fluid and $\nabla\mathbf{V}$ the velocity gradient, defined as $[\nabla\mathbf{V}]_{ij} = \frac{\partial V_i}{\partial x_j}$. Throughout the paper we assume viscosity μ to be constant everywhere. Formula (1) combines two clearly distinct physical effects. On the one hand there is the contribution of the viscous stresses $\bar{\bar{\Pi}}_{\mu} \cdot \mathbf{n}$, which are defined locally. This means that given the velocity field, which is itself a non-local quantity, they can be obtained by computing the velocity derivatives, and therefore the accuracy of this operation principally depends on the resolution in the proximity of the boundary. On the other hand, pressure p is non-local in that its value at a particular point depends on velocity and vorticity fields in the whole flow domain. This makes evaluation of $\mathbf{F}^{\mathrm{P}}$ more difficult, especially in the case of open flow systems. Furthermore, application of formula (1) is particularly inconvenient when the hydrodynamic problem is cast in terms of the non-primitive variables, i.e., the momentum equation is expressed in the velocity–vorticity (or streamfunction–vorticity) rather than the velocity–pressure form [2]. In this case pressure may only be obtained as a solution of a separate problem [3]. Consequently, efficient computation of the pressure contribution to the hydrodynamic force may in some cases cause problems. At the same time it is well known that in many important flow configurations, e.g., bluff body wakes, its contribution to the total force is dominating.

An alternative approach consists in using the *vorticity impulse* relation [4] and yields

$$\mathbf{F} = -\frac{1}{D-1}\frac{d}{dt}\int_{\Omega} \mathbf{r} \times \boldsymbol{\omega}\, d\Omega + \frac{d}{dt}\oint_{\partial\Omega} \mathbf{r} \times (\mathbf{n} \times \mathbf{V})\, d\sigma, \qquad (3)$$

where $\mathbf{r}$ denotes the position vector and D is the spatial dimension ($D = 2$ or $D = 3$). In the above Ω is the flow domain extending to infinity. This formula does not explicitly refer to the pressure information. From the computational point of view it has, however, a number of shortcomings. In the first place it involves numerical differentiation resulting in a noisy signal, particularly when a low-order time stepping scheme is used. Furthermore, it has the disadvantage that vorticity in the near and far wake contribute equally to the hydrodynamic force [5]. This approach was recently revisited in [6] and [7], where the momentum balance in some finite control volume (CV) surrounding the body was considered. A family of relations was derived, all of them having the structure

$$\mathbf{F} = -\frac{1}{D-1}\frac{d}{dt}\int_{\mathrm{CV}} \mathbf{r} \times \boldsymbol{\omega}\, d\Omega + \{\text{integral over the outer surface of the CV}\}$$

$$+ \{\text{integral over the body surface}\}. \qquad (4)$$

In this case, as well, time differentiation is required to compute force. Furthermore, using the formulas (3) and (4), one is not able to separate the contributions of pressure and viscous stresses, which might be desirable in some applications.

It is thus of much practical and theoretical importance to develop an approach which will alleviate the above difficulties. We will extend the variational procedure originally presented in [1] and derive a formula for the pressure force which does not refer to pressure

information and uses only velocity and vorticity fields. Furthermore, it does not involve time differentiation, apart from the time derivative of a boundary term. The latter, however can be computed using the data prescribed in the statement of the problem. At the same time, the contribution of vorticity to the force is taken with a weight diminishing with the distance from the obstacle. In order to obtain the total force it will only be necessary to supplement the term representing the viscous stresses.

2. HYDRODYNAMIC FORCE—VARIATIONAL APPROACH

In this section we will present the derivation of the formula that allows one to compute the pressure force in a convenient manner. We will first transform the relation (1). To this end we will use the identity of vector calculus

$$\oint_{\partial\Omega} (\nabla \mathbf{V})^{\mathrm{T}} \cdot \mathbf{n} \, d\sigma = \int_{\Omega} \nabla(\nabla \cdot \mathbf{V}) \, d\Omega, \tag{5}$$

where $[(\nabla \mathbf{V})^{\mathrm{T}} \cdot \mathbf{n}]_i = \frac{\partial V_j}{\partial x_i} n_j$ (summation is implied when indices are repeated). The above integrals vanish when the field $\mathbf{V}$ is divergence-free. This relation holds for any body with shape changing in time. Using this property along with (1) and (2) one can show that the well-known formula

$$\mathbf{F} = \oint_{\partial\Omega} [p\mathbf{n} - \mu(\nabla \mathbf{V} + (\nabla \mathbf{V})^{\mathrm{T}}) \cdot \mathbf{n}] \, d\sigma = \oint_{\partial\Omega} [p\mathbf{n} - \mu(\nabla \mathbf{V} - (\nabla \mathbf{V})^{\mathrm{T}}) \cdot \mathbf{n}] \, d\sigma$$

$$= \oint_{\partial\Omega} (p\mathbf{n} + \mu\mathbf{n} \times \boldsymbol{\omega}) \, d\sigma \tag{6}$$

remains valid for any body with time dependent shape $\partial\Omega = \partial\Omega(t)$.

Following the idea originally presented in [1], we consider the region Ω which is the exterior of the body. It is bounded by two surfaces (curves in the plane case): Γ_0, which coincides with the body surface, and Γ_1, which is the outer circumference. Now we define the function η_x so that

$$\triangle \eta_x = 0 \quad \text{in } \Omega$$
$$\mathbf{n} \cdot \nabla \eta_x|_{\Gamma_0} = -\mathbf{e}_x \cdot \mathbf{n} \tag{7}$$
$$\mathbf{n} \cdot \nabla \eta_x|_{\Gamma_1} = 0,$$

where $\mathbf{e}_x$ is the versor of the X-axis in the Cartesian coordinate system. The function η_x is thus the solution of the Neumann problem for the Laplace equation. The solvability condition is $\oint_{\Gamma_0} \mathbf{e}_x \cdot \mathbf{n} \, d\sigma = 0$ and it is straightforward to verify that it is satisfied. The solution is defined up to an additive constant, which will be adjusted below, and has the property that for large distances r it behaves like $O(\frac{1}{r})$ in 2D and $O(\frac{1}{r^2})$ in 3D. The function η_x will be used to determine the X-component of the pressure force $\mathbf{F}^{\mathrm{P}}$. In order to obtain the other components (F_y^{P} and F_z^{P}), the corresponding functions η_y and η_z will have to be introduced. They are defined by a problem similar to (7) with the boundary condition on Γ_0 replaced by $-\mathbf{e}_y \cdot \mathbf{n}$ and $-\mathbf{e}_z \cdot \mathbf{n}$, accordingly. In the following considerations we will focus on the drag force F_x. First we express the pressure term $-\nabla p$ using the Navier–Stokes equation (with density ρ set equal to unity)

$$-\nabla p = \frac{\partial \mathbf{V}}{\partial t} + (\mathbf{V} \cdot \nabla)\mathbf{V} + \mu\nabla \times \boldsymbol{\omega}. \tag{8}$$

It is then projected (in the sense of the Hilbert space $L_2(\Omega)$) on the gradient $\nabla \eta_x$. Each term in Eq. (8) is multiplied by $\nabla \eta_x$ and then integrated over Ω. Integrating by parts, using the incompressibility constraint and the boundary conditions for η_x we obtain [1]

$$F_x^{\mathrm{P}} = \oint_{\Gamma_0} (n_x \, p) \, d\sigma = \oint_{\Gamma_0 \cup \Gamma_1} \eta_x \mathbf{n} \cdot \left(\frac{\partial \mathbf{V}}{\partial t} \right) d\sigma + \mu \oint_{\Gamma_0 \cup \Gamma_1} \mathbf{n} \cdot (\boldsymbol{\omega} \times \nabla \eta_x) \, d\sigma$$
$$+ \int_{\Omega} \nabla \eta_x \cdot [(\mathbf{V} \cdot \nabla) \mathbf{V}] \, d\Omega, \tag{9}$$

where $n_x = \mathbf{e}_x \cdot \mathbf{n}$. Note that even though the above relation represents the pressure force, one of the boundary terms involves viscosity. In this work we consider general boundary shapes, including those with geometric singularities (i.e., corners). In that case the unit normal vector may be discontinuous, with its value at singular points equal to the mean of the two limits. This is, however, not a problem, since (7) can be solved in the weak sense, whereas in all the remaining cases $\mathbf{n}$ appears in integrand expressions.

For the sake of simplicity we will now restrict ourselves to the two-dimensional (2D) case; the extension to 3D is, however, straightforward. We will therefore use the term *contour* instead of *body* and denote $\omega = \omega_z$ (all the remaining vorticity components vanish). In order to further simplify the relation we introduce the following assumptions:

- place the outer perimeter Γ_1 at infinity ($\Gamma_1 \to \Gamma_\infty$); consequently, at infinity η_x falls off to a constant which will be set equal to zero,
- assume that for any finite time $0 < t < \infty$ vorticity vanishes at infinity like $\omega \sim e^{-r^2}$; this is true for all the flows in which the initial vorticity has compact support, as in finite time advection cannot take vorticity to infinity and the above asymptotic formula is consistent with the properties of the diffusion equation (this category comprises all the flows of interest),
- in the 2D case assume that the difference between velocity and the free stream $\|\mathbf{V} - \mathbf{V}_\infty\|$ decays at infinity like $O(\frac{1}{r^2})$; this assumption implies that $\int_\Omega \omega \, d\Omega + \oint_{\Gamma_0} \mathbf{V} \cdot \mathbf{t} \, d\sigma = 0$ and that there is no net circulation in the flow domain, and in fact this is a necessary constraint on plane flows, since otherwise the part of the kinetic energy associated with vortical motion of the fluid would not be finite [8].

It must be observed that none of the above assumptions is restrictive. In the derivation below we will exploit the asymptotic properties of integrals taken over the contour Γ_∞. Here we remark that such integrals vanish when their integrand expressions decay like $O(\frac{1}{r^{2+\epsilon}})$ with $\epsilon > 0$. It is now possible to carry out further simplifications. The non-linear term in (9) transforms as follows:

$$\int_{\Omega} \nabla \eta_x \cdot [(\mathbf{V} \cdot \nabla) \mathbf{V}] \, d\Omega = \int_{\Omega} \nabla \eta_x \cdot \left[\nabla \frac{V^2}{2} - \mathbf{V} \times \omega \mathbf{k} \right] d\Omega$$
$$= \int_{\Omega} \nabla \cdot \left(\frac{V^2}{2} \nabla \eta_x \right) d\Omega - \int_{\Omega} \nabla \eta_x \cdot (\mathbf{V} \times \omega \mathbf{k}) \, d\Omega$$
$$= \oint_{\Gamma_0} (\mathbf{n} \cdot \nabla \eta_x) \frac{V^2}{2} \, d\sigma + \oint_{\Gamma_\infty} (\mathbf{n} \cdot \nabla \eta_x) \frac{V^2}{2} \, d\sigma - \int_{\Omega} \nabla \eta_x \cdot (\mathbf{V} \times \omega \mathbf{k}) \, d\Omega$$
$$= -\oint_{\Gamma_0} n_x \frac{V^2}{2} \, d\sigma - \int_{\Omega} \nabla \eta_x \cdot (\mathbf{V} \times \omega \mathbf{k}) \, d\Omega. \tag{10}$$

The integral over Γ_∞ vanishes due to the external boundary conditions for $\mathbf{n} \cdot \nabla \eta_x$ (Eq. (7)). In Eq. (9) there are two integrals that are taken over the outer perimeter. The one involving the viscous term ($\mu \oint_{\Gamma_\infty} \mathbf{n} \cdot (\omega \times \nabla \eta_x) \, d\sigma$) vanishes because of the rapid decay of ω and η_x at infinity. The other one can be transformed using the asymptotic representation for the velocity field far from the obstacle,

$$\mathbf{V} = \mathbf{V}_\infty(t) + \frac{\mathbf{c}(t)}{r^2} + O\left(\frac{1}{r^3}\right), \tag{11}$$

which is consistent with the third assumption introduced above. The term in question now becomes

$$\oint_{\Gamma_\infty} \mathbf{n} \cdot \left(\frac{\partial \mathbf{V}}{\partial t}\right) \eta_x \, d\sigma = \frac{du_\infty}{dt} \oint_{\Gamma_\infty} n_x \eta_x \, d\sigma + \frac{dv_\infty}{dt} \oint_{\Gamma_\infty} n_y \eta_x \, d\sigma + O\left(\frac{1}{r^2}\right). \tag{12}$$

The derivatives $\frac{du_\infty}{dt}$ and $\frac{dv_\infty}{dt}$ represent the accelerations of the free stream components $\mathbf{V}_\infty = [u_\infty; v_\infty]$ and thus correspond to the added mass effect (in fact, this effect is also represented by the analogous term taken on the contour Γ_0). In the next section we will derive closed formulas for the integrals $\oint_{\Gamma_\infty} n_x \eta_x \, d\sigma$ and $\oint_{\Gamma_\infty} n_y \eta_x \, d\sigma$. As a result the pressure drag force is given by

$$F_x^{\mathrm{P}} = -\int_\Omega \nabla \eta_x \cdot (\mathbf{V} \times \omega \mathbf{k}) \, d\Omega + \mu \oint_{\Gamma_0} \nabla \eta_x \cdot (\mathbf{n} \times \omega \mathbf{k}) \, d\sigma + \oint_{\Gamma_0} \mathbf{n} \cdot \left(\frac{\partial \mathbf{V}}{\partial t}\right) \eta_x \, d\sigma$$
$$- \oint_{\Gamma_0} n_x \frac{V^2}{2} \, d\sigma + \frac{du_\infty}{dt} \oint_{\Gamma_\infty} n_x \eta_x \, d\sigma + \frac{dv_\infty}{dt} \oint_{\Gamma_\infty} n_y \eta_x \, d\sigma. \tag{13}$$

We can now supplement the contribution of the viscous stresses $F_x^\mu = \mu \mathbf{e}_x \cdot \oint_{\Gamma_0} \mathbf{n} \times \omega \mathbf{k} \, d\sigma$, which can be collapsed into the first boundary term and we finally obtain the expression for the total drag force,

$$F_x = -\int_\Omega \nabla \eta_x \cdot (\mathbf{V} \times \omega \mathbf{k}) \, d\Omega + \mu \oint_{\Gamma_0} (\mathbf{n} \times \omega \mathbf{k}) \cdot (\nabla \eta_x + \mathbf{e}_x) \, d\sigma + \oint_{\Gamma_0} \mathbf{n} \cdot \left(\frac{\partial \mathbf{V}}{\partial t}\right) \eta_x \, d\sigma$$
$$- \oint_{\Gamma_0} n_x \frac{V^2}{2} \, d\sigma + \frac{du_\infty}{dt} \oint_{\Gamma_\infty} n_x \eta_x \, d\sigma + \frac{dv_\infty}{dt} \oint_{\Gamma_\infty} n_y \eta_x \, d\sigma. \tag{14}$$

As opposed to the standard approaches discussed in the Introduction, the derived formula does not involve time differentiation of the field quantities, except for the time derivative of the boundary velocity. The latter is, however, the boundary condition for the Navier–Stokes system and as such does not have to be calculated separately. Furthermore, the integrand expression in the area integral in (14) is multiplied by the weighing factor $\nabla \eta_x$, which decays like $O(\frac{1}{r^2})$. Consequently, the contribution of the vorticity far downstream is much smaller than that of the vorticity in the near wake. These are important computational advantages over the formulas (3) and (4). In some particular cases the formula (14) may be further simplified. For example, the term involving the time derivative of the boundary velocity vanishes when the contour has circular symmetry, or when there is no angular acceleration. In the case of solid body rotation the fourth term can be transformed using the Green's

theorem

$$\oint_{\Gamma_0} n_x \frac{V^2}{2} \, d\sigma = \oint_{\Gamma_0} n_x \frac{\dot{\varphi}^2 r^2}{2} \, d\sigma = \frac{\dot{\varphi}^2}{2} \oint_{\Gamma_0} n_x (x^2 + y^2) \, d\sigma$$

$$\frac{\dot{\varphi}^2}{2} \int_A \frac{\partial}{\partial x} (x^2 + y^2) \, dA = \dot{\varphi}^2 \int_A x \, dA,$$

(15)

where A stands for the area of the contour and $\dot{\varphi}$ is the rotational velocity. This implies that the term vanishes when the contour rotates about its center of mass, for the X and Y directions, respectively. As a result, when the obstacle is a fixed cylinder, or a rotating circular cylinder, then the formula (14) consists of the first two integrals only plus the terms corresponding to the free stream acceleration.

3. DETERMINATION OF THE FUNCTION η_x

To take advantage of formulas (13) and (14) it is necessary to compute the function gradient $\nabla \eta_x$ (correspondingly $\nabla \eta_y$) in the domain Ω and the value both of η_x and of its gradient $\nabla \eta_x$ on the boundary $\partial \Omega$. As the solution of an external Neumann problem (7), the function η_x can be obtained in a number of different ways. In the following we will describe a method which is particularly suitable when the velocity and vorticity fields are computed using a vortex approach. In that case the area integral in (14) simply reduces to a quadrature over the vorticity carriers (*vortex blobs*), their number being relatively high ($O(10^5–10^6)$). At every instant of time it will therefore be necessary to evaluate $\nabla \eta_x$ at a different set of points corresponding to the locations of the vortex blobs with ever increasing distance from the obstacle. Thus standard techniques based on an a priori evaluation of η_x and $\nabla \eta_x$ on a fixed grid in Ω are inconvenient. We will now present an alternative approach.

In the flow domain Ω the harmonic function η_x can be represented using Green's formula. In the 2D case it takes the form

$$\eta_x(X) = \frac{1}{2\pi} \oint_{\partial \Omega} \eta_x(Q) \frac{\cos(\mathbf{n}_Q, \mathbf{XQ})}{|\mathbf{XQ}|} \, d\sigma - \frac{1}{2\pi} \oint_{\partial \Omega} (\mathbf{n} \cdot \nabla \eta_x) \ln|\mathbf{XQ}| \, d\sigma$$

$$X \in \Omega, \, Q \in \partial \Omega. \quad (16)$$

The integrals in the above formula are taken over the contour boundary. The function $\eta_x(Q)$ can be obtained using the boundary integral equation

$$\eta_x(P) + \frac{1}{\pi} \oint_{\partial \Omega} \eta_x(Q) \frac{\cos(\mathbf{n}_Q, \mathbf{PQ})}{|\mathbf{PQ}|} \, d\sigma = \frac{1}{\pi} \oint_{\partial \Omega} (\mathbf{n} \cdot \nabla \eta_x) \ln|\mathbf{PQ}| \, d\sigma \quad P, \, Q \in \partial \Omega. \quad (17)$$

This is the Fredholm equation of the second kind and can be solved using standard techniques. The integrand expression on the right hand side in (17) can be evaluated using the boundary condition from (7). In order to extend this approach to the spatial case, the corresponding 3D versions of the kernel functions have to be substituted into (16) and (17). The gradient $\nabla \eta_x$ can be calculated by applying integration by parts to the formula (16),
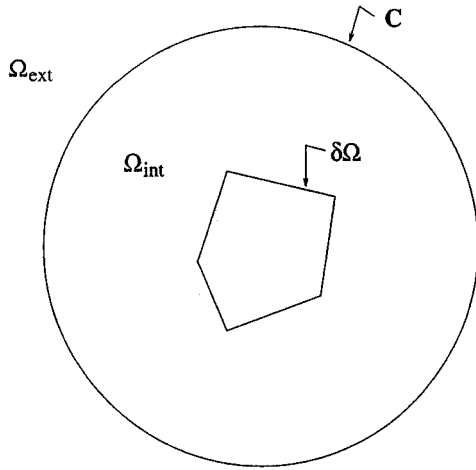
FIG. 1.   Schematic division of the computational domain into Ω_{int} and Ω_{ext}.

$$\nabla \eta_x(X) = \frac{1}{2\pi} \oint_{\partial\Omega} \eta_x(Q) \frac{\mathbf{n}_Q - 2\mathbf{q}\cos(\mathbf{n}_Q, \mathbf{XQ})}{|\mathbf{XQ}|^2} \, d\sigma + \frac{1}{2\pi} \oint_{\partial\Omega} (\mathbf{n} \cdot \nabla \eta_x) \frac{\mathbf{XQ}}{|\mathbf{XQ}|^2} \, d\sigma,$$

$$X \in \Omega, \, Q \in \partial\Omega, \quad (18)$$

where $\mathbf{q} = \frac{\mathbf{XQ}}{|\mathbf{XQ}|}$. Using vortex methods, the above formula has to be independently evaluated for every single vorticity carrier, i.e., as many as $O(10^5\text{--}10^6)$ times at every time step. This is computationally intensive and therefore application of (18) is not convenient, especially far from the contour where the variation of the function η_x is fairly slow.

To avoid this we will use a hybrid approach. We introduce a circle C (a sphere in the 3D case) with the diameter D_C significantly larger then the characteristic dimension of the obstacle. As shown in Fig. 1, the computational domain is thus split into two ($\Omega_{\text{int}} \cup \Omega_{\text{ext}} = \Omega$):

• the interior annular region Ω_{int} between the obstacle and the circle C; in this domain the function η_x varies fairly rapidly and the solution of the Neumann problem (7) is obtained using a finite element method (FEM) on a refined mesh,

• the region Ω_{ext} external to the circle C where the function η_x is varying fairly slowly; the function η_x is represented there as a Laurent series with rapidly decaying coefficients; the expansion is determined by matching the two solutions on the circle C.

Consequently, evaluation of η_x or $\nabla \eta_x$ requires only either interpolation from the fixed grid (in the case of $X \in \Omega_{\text{int}}$), or summation of the power series with a small number of terms (in the case of $X \in \Omega_{\text{ext}}$). Even though there is some overhead cost related to the solution of the problem in Ω_{int} and then determining the expansion coefficients in Ω_{ext}, the presented method results in significant speed-up comparing with the approach based on formulas (16) and (18). Furthermore, it should be remarked that when the contour does not change in time, the overhead calculations are performed once for all. Details for the solutions of the problem in Ω_{int} and Ω_{ext} are given below.

3.1. *Solution of the Internal Problem*

The Neumann problem in the region Ω_{int} can be solved using, for example, the weak formulation. The boundary condition on Γ_0 follows from (7), whereas the boundary condition on C can be generated using the formula (18). This, however, requires that the additional

boundary value problem (17) be solved beforehand. Nevertheless, in certain implementations of the vortex method (e.g., [9]), an analogous problem has to be solved in order to determine the potential component of the velocity field. Consequently, in these two steps the same inverse matrix can be used, resulting in significant reduction of the overhead cost related to matrix inversion. As mentioned above, the solution of an external Neumann problem is defined up to an additive constant. Below we will show how to fix this constant so that the solution will correspond to the function η_x vanishing at infinity.

3.2. Solution of the External Problem

In the exterior Ω_{ext} of the circle C the harmonic function η_x can be represented as the Laurent series

$$\eta_x(x, y) = \Re\left(\sum_{k=0}^{\infty} \frac{a_k}{z^k}\right) = \sum_{k=0}^{\infty} \left(\frac{R_C}{r}\right)^k [\alpha_k \cos(k\varphi) + \beta_k \sin(k\varphi)], \tag{19}$$

where $z = x + iy$ (i is the imaginary unit), R_C is the radius of the circle C, (r, φ) are the polar coordinates of the point (x, y), and $\Re$ denotes the real part of a complex number. The numbers $\{\alpha_k, \beta_k\}_{k=0}^{\infty}$ are the expansion coefficients. They can be determined by performing spectral (in terms of Fourier harmonics) analysis of the function $\eta_x(R, \varphi) = \tilde{\eta}_x(\varphi)$ computed on the circle C. In this evaluation the solution in Ω_{int} can be used.

We will now adjust the indeterminate constant that appears in the solution of the Neumann problem. It is equal to the zeroth term in the expansion (19),

$$\alpha_0 = \int_0^{2\pi} \tilde{\eta}_x(\varphi') \, d\varphi', \tag{20}$$

and is subtracted from the final solution. In fact the expansion coefficients decay very rapidly and only a small number N of terms have to be retained to ensure the desired accuracy. In the 3D case the function η_x is expanded in terms of spherical harmonics $P_l^k(\cos(\theta))$,

$$\eta_x(x, y, z) = \sum_{k,l=0}^{\infty} \gamma_{kl} P_l^k(\cos(\theta)) e^{ik\varphi} \left(\frac{R_C}{r}\right)^{l+1}, \tag{21}$$

where (r, θ, φ) are the spherical coordinates of the point (x, y, z). As before, the expansion coefficients are determined by performing spherical harmonic analysis. The additional condition is also similar:

$$\gamma_{0,0} = \int_0^{2\pi} \int_0^{\pi} \eta_x(\theta', \varphi') \sin(\theta') \, d\theta' \, d\varphi'. \tag{22}$$

Using the representation (19) for the function η_x we are now able to evaluate the integrals in (12),

$$\oint_{\Gamma_\infty} n_x \eta \, d\sigma = \lim_{r \to \infty} \int_0^{2\pi} \cos(\varphi) \eta(\varphi) r \, d\varphi$$

$$= \lim_{r \to \infty} \left[R_C \int_0^{2\pi} \cos(\varphi) \frac{\alpha_1 \cos(\varphi) + \beta_1 \sin(\varphi)}{r} r \, d\varphi + O\left(\frac{1}{r}\right) \right]$$

$$= \pi R_C \alpha_1, \tag{23}$$

where η_x or η_y should be substituted for η. Only the term corresponding to $k = 1$ has a non-vanishing contribution to the integral.

4. EXAMPLE CALCULATIONS

In this section we present computational examples concerning the determination of the functions η_x and η_y, and subsequent evaluation of the hydrodynamic force for some simple flow configurations. In the simplest case, when the obstacle is a circular cylinder, the solution is available in the analytical form. It is straightforward to verify that then $\eta_x(r, \theta) = R_0^2 \frac{\cos(\theta)}{r}$, $\eta_y(r, \theta) = R_0^2 \frac{\sin(\theta)}{r}$, and $\nabla \eta_x(r, \theta) = -\frac{R_0^2}{r^2}[\cos(2\theta), \sin(2\theta)]^{\mathrm{T}}$, $\nabla \eta_y(r, \theta) = -\frac{R_0^2}{r^2}[\sin(2\theta), -\cos(2\theta)]^{\mathrm{T}}$. These relations can be used to verify the accuracy of the algorithm which is implemented to calculate the function η.

One should observe that when the contour rotates without any change of shape, determination of η_x and η_y can be considerably simplified. Rotation of the contour by the angle α implies that in the local frame of reference, denoted $X^\alpha O Y^\alpha$, the global frame XOY is rotated by the angle $-\alpha$ (Fig. 2). Let the superscript α denote quantities referred to the local (i.e., rotated) frame of reference and 0 those expressed in the fixed frame. The boundary conditions for the problem (7) represent the projections n_x^0 and n_y^0 of the unit normal $\mathbf{n}$ on the axes X and Y of the global reference system for the case of η_x and η_y, respectively. Since the contour does not deform, the corresponding projections n_x^α and n_y^α remain unchanged, and so do the solutions η_x^α and η_y^α in the local coordinate system. The projections n_x^0 and n_y^0 can therefore be expressed in terms of n_x^α and n_y^α in the following way:

$$n_x^0 = n_x^\alpha \cos(\alpha) + n_y^\alpha \sin(\alpha)$$
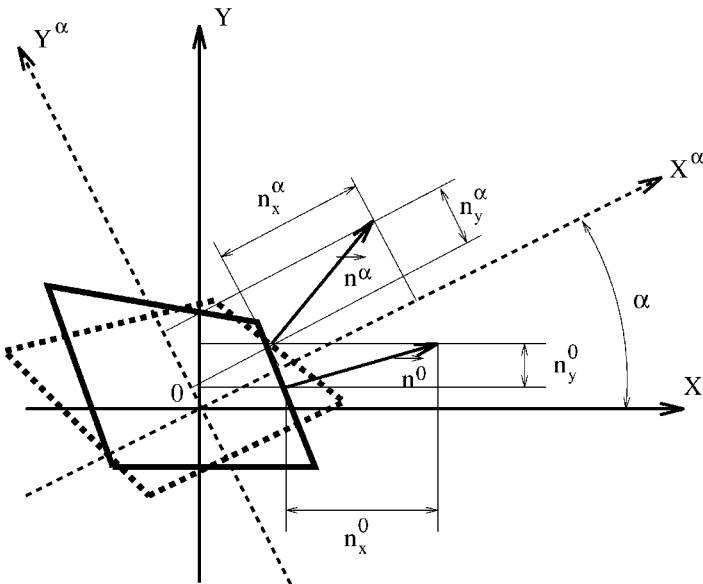$$n_y^0 = -n_x^\alpha \sin(\alpha) + n_y^\alpha \cos(\alpha). \tag{24}$$

FIG. 2. Representation of the boundary condition for the problem (7) in the fixed (solid line) and rotated (dashed line) frames of reference.
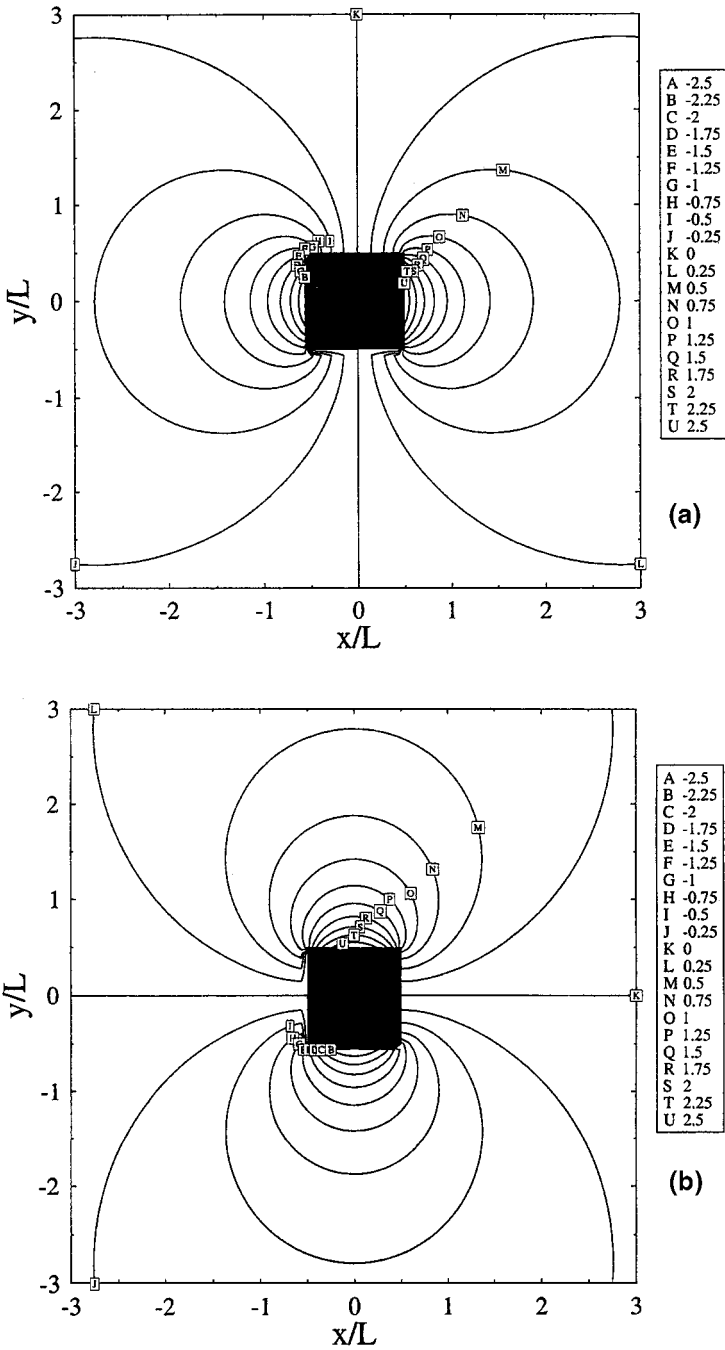
FIG. 3.   Isolines of the function η_x (a) and η_y (b) for the case of the square cylinder.

Consequently, using linearity of the Neumann problem with respect to the boundary conditions, the functions η_x^0 and η_y^0 can be represented as

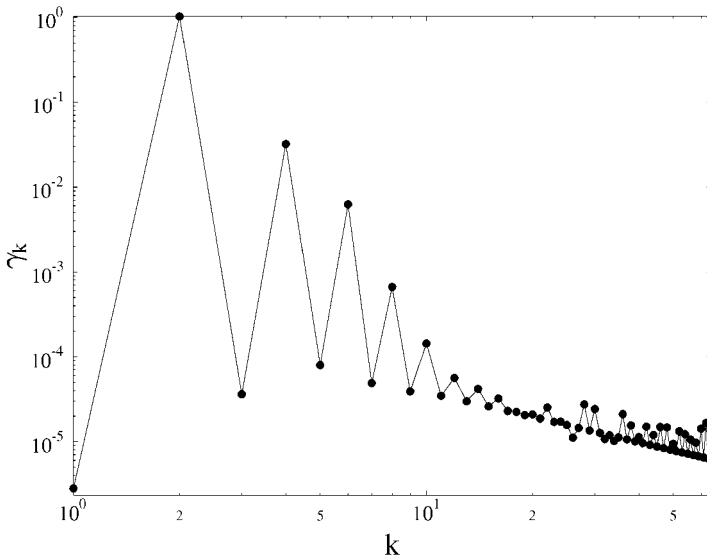$$\eta_x^0 = a\eta_x^\alpha - b\eta_y^\alpha$$
$$\eta_y^0 = b\eta_x^\alpha + a\eta_y^\alpha,$$

(25)

FIG. 4. The amplitudes of the coefficients $\gamma_k = \sqrt{\alpha_k^2 + \beta_k^2}$ the expansion (19) as a function of the index k for the case of the square cylinder (they are the same for both η_x and η_y).

where $a = \cos(\alpha)$ and $b = -\sin(\alpha)$. These are the functions that should be used in the relations (9) through (14). Consequently, for any rotation angle α, the solutions η_x^0 and η_y^0 can be recovered as a linear combination of the reference solutions η_x^α and η_y^α with the coefficients depending on the rotation angle. This significantly reduces the overhead cost in the situation where the contour rotates as a solid body.

In Fig. 3 we show the isolines of η_x and η_y for the case of the square cylinder. The circle C has the radius $R_C = 3\frac{L}{2}$, where L is the characteristic dimension of the obstacle. The internal problem was solved using a second-order accurate finite element method with roughly 16,000 elements. In the computation of the external solution $N = 64$ terms were used. In Fig. 4 we present the log–log plots of the magnitudes of the expansion coefficients $\gamma_k = \sqrt{\alpha_k^2 + \beta_k^2}$ as a function of the wavenumber k (the plots are the same for both η_x and η_y). Note the rapid decay of the coefficients.

Since in this work we are mainly concerned with the derivation of an efficient formula for the pressure force, we begin the presentation of our results with the time evolution of the pressure drag and pressure lift coefficients, defined as $c_D^P = F_x^P / \frac{U_\infty^2 L}{2}$ and $c_L^P = F_y^P / \frac{U_\infty^2 L}{2}$, respectively. They were computed for the 2D wake flow past a square cylinder (Figs. 5a and 6a). The Reynolds number $\text{Re} = \frac{U_\infty L}{\nu}$ was equal to 1000. In Figs. 7a and 8a we show the same parameters obtained in the case when the obstacle was rotating with the normalized angular velocity $\frac{\dot{\varphi} L}{U_\infty} = 0.5$. For the purpose of verification the coefficients c_D^P and c_L^P presented in Figs. 5a through 8a were computed using two different methods: (i) the formula (13) and (ii) integration of the pressure distribution on the contour. All the simulations were performed using the random vortex blob method described in [9] with the number of vorticity carriers being on the order of 10^5. Pressure on the contour was determined using a finite element method to solve the weak form of Eq. (8). The solution method is described in [3]. In Figs. 5b through 8b we show the time evolution of the total drag and lift coefficients for the same flow configurations. Again the coefficients $c_D = F_x / \frac{U_\infty^2 L}{2}$ and $c_L = F_y / \frac{U_\infty^2 L}{2}$ are computed in two different ways: (i) by applying formula (14), and (ii) by using the
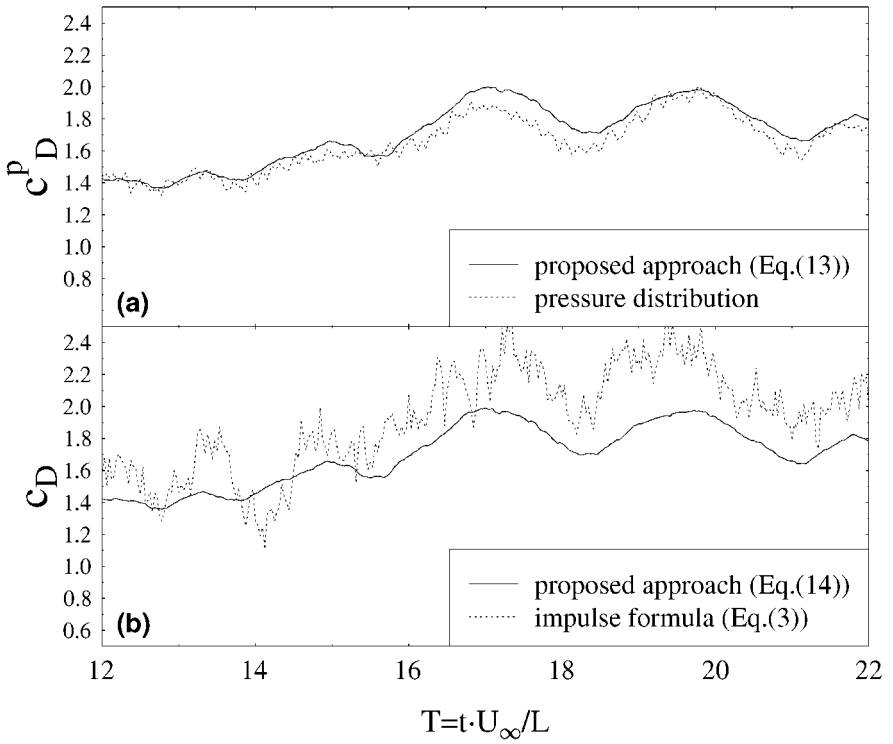
FIG. 5. Time histories of the pressure drag (top) and the total drag (bottom) coefficients c_D^p and c_D for the wake flow past a square cylinder at Re = 1000. The coefficients are computed using different methods (see insets).
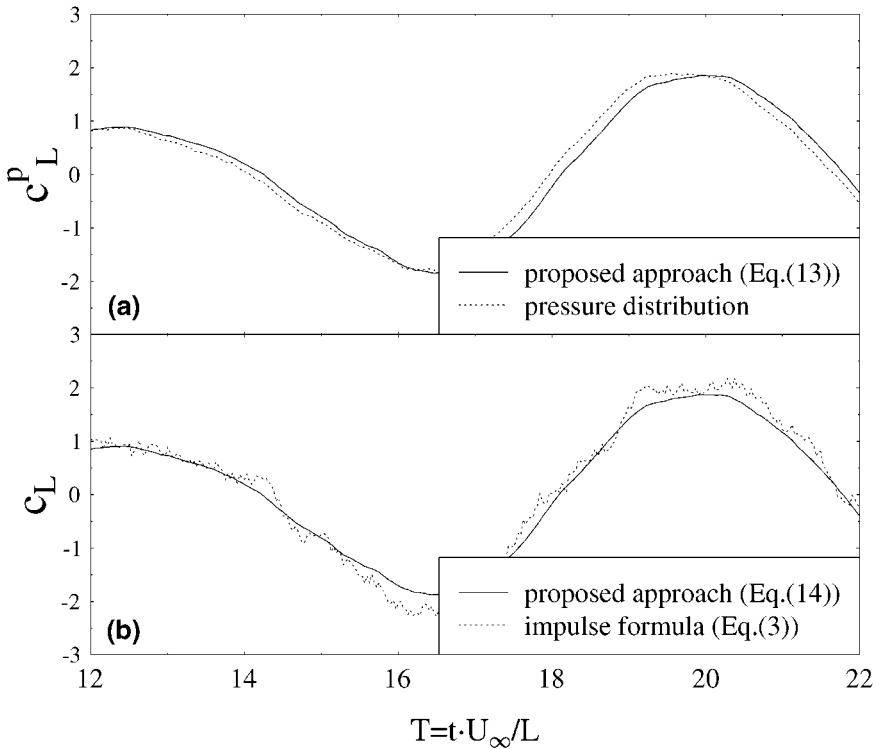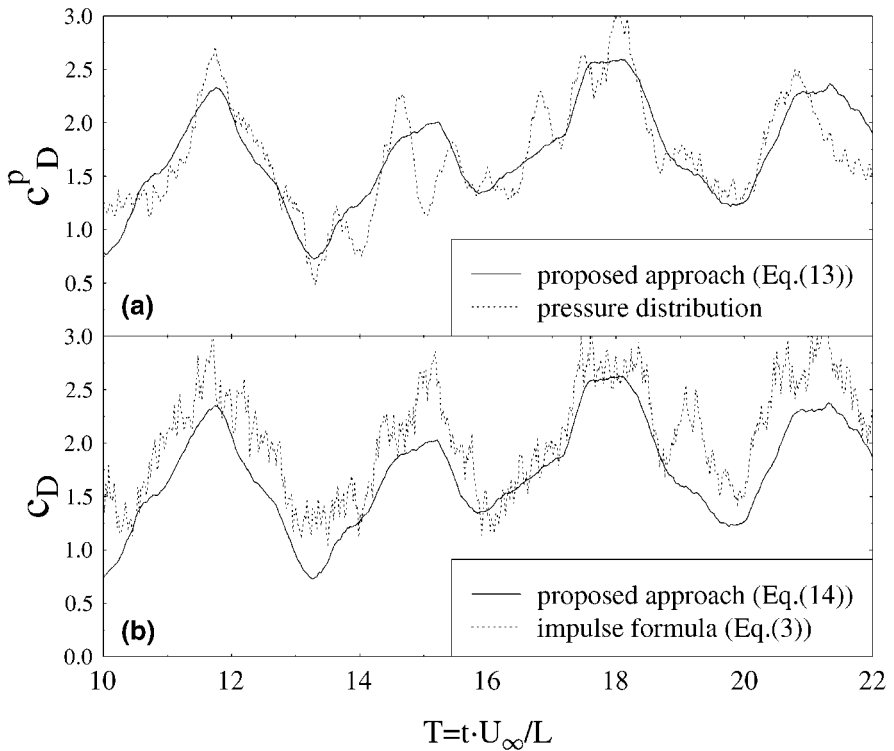

FIG. 6. Time histories of the pressure lift (top) and the total lift (bottom) coefficients c_L^p and c_L for the wake flow past a square cylinder at Re = 1000. The coefficients are computed using different methods (see insets).

FIG. 7. Time histories of the pressure drag (top) and the total drag (bottom) coefficients c_D^P and c_D for the wake flow past a rotating square cylinder at $Re = 1000$ and the normalized rotational velocity $\frac{\dot{\phi}L}{U_\infty} = 0.5$. The coefficients are computed using different methods (see insets).

impulse relation (3). Because of noise, the signals had to be artificially smoothed, which was done by performing running averages over 15 adjacent samples in all cases. Nevertheless, the signals obtained using the impulse formula (3) still remain irregular, thus implying a much higher level of noise.

As a first remark one should mention the very good agreement between the pressure and the total lift coefficients c_L^P and c_L obtained using different methods in both flow configurations (Figs. 6 and 8). The agreement is slightly worse as regards the total drag c_D (Figs. 5b and 7b). The reason for this is the effect of the viscous force $\mathbf{F}^\mu$, which contributes to the drag force while having no net effect on the lift. Consequently, evaluation of the former depends on the details of the boundary layer, which may have not been sufficiently resolved in the simulations. The impulse formula (3) does not explicitly refer to the boundary layer information, and therefore the discrepancies observed in Figs. 5b and 7b may be attributed to the inaccuracy related to evaluation of $\mathbf{F}^\mu$. This conclusion is also confirmed by the good agreement obtained for the pressure drag coefficients c_D^P (Figs. 5a and 7a). The irregular behavior of the pressure drag coefficient c_D^P computed using the pressure surface distribution may be caused by the finite domain effects involved in its determination. As already remarked, pressure is computed using a grid-based solver, and the effect of the vorticity which is outside the computational domain is represented by suitable boundary terms. The influence that truncation of the computational domain may have on the calculated force was discussed in [7]. Finally, it should be stressed that in all
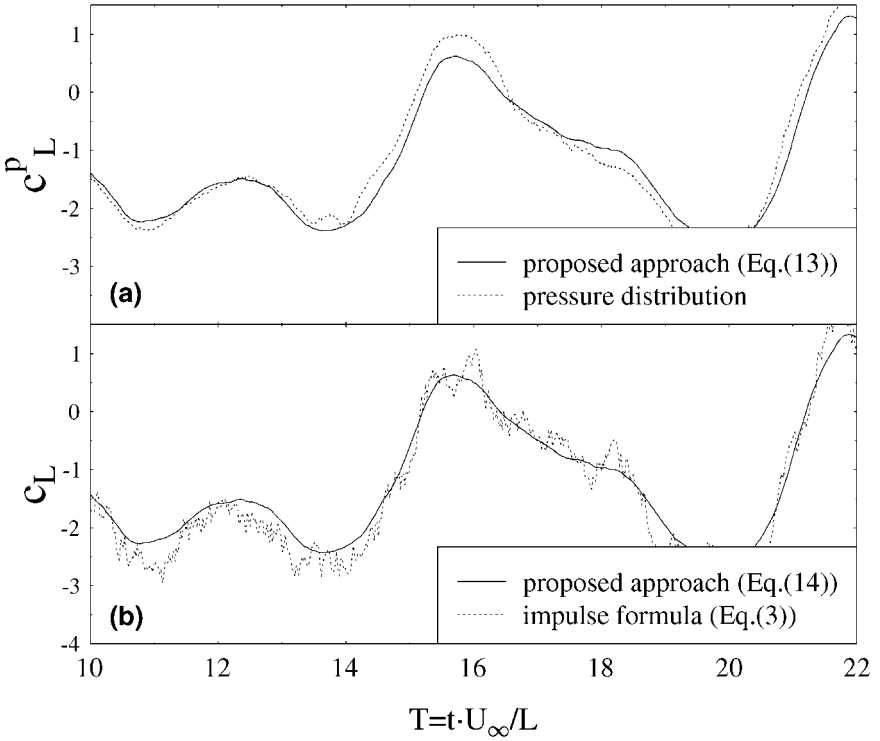
FIG. 8. Time histories of the pressure lift (top) and the total lift (bottom) coefficients c_L^P and c_L for the wake flow past a rotating square cylinder at $Re = 1000$ and the normalized rotational velocity $\frac{\dot{\psi}L}{U_\infty} = 0.5$. The coefficients are computed using different methods (see insets).

the cases the proposed formulas (13) and (14) resulted in signals which were much more regular than those obtained by the other methods.

5. CONCLUSIONS

In the present paper we have derived an efficient formula for the computation of the pressure forces in hydrodynamics. It is a variational approach based on velocity and vorticity fields and is therefore particularly well suited for the case when a vortex method is used to solve the flow problem. The total force can be recovered by supplementing the viscous term $\mathbf{F}^\mu$. Our formula is robust and comparing to the standard techniques based on (3) exhibits a number of computational advantages. In the first place it does not involve time differentiation which means that good results may be obtained with low order time stepping schemes. Additionally, the contribution of vorticity diminishes with the distance from the obstacle which is due to the presence of the factor $\nabla\eta$ decaying like $O(\frac{1}{r^2})$. As a result, the loss of accuracy related to particle merging or core spreading performed far downstream in certain implementations of the vortex method (e.g., [5]) will not significantly influence the computation of forces. Within the new approach it is required that a family of the harmonic functions η should be available. They are the solutions of the Neumann problem for the Laplace equation and as such can be readily computed. A convenient method for their evaluation is also proposed. The formula (14) has however the disadvantage that it

involves the boundary value of vorticity. Consequently, the obtained results may depend on the details of boundary layer resolution, particularly for the drag force.

ACKNOWLEDGMENTS

REFERENCES

1. L. Quartapelle and M. Napolitano, Force and moment in incompressible flows, *AIAA J.* **21**(6), 911 (1983).

2. P. M. Gresho, Incompressible fluid dynamics: Some fundamental formulation issues, *Annu. Rev. Fluid Mech.* **23**, 413 (1991).

3. A. Nowakowski, J. Rokicki, and A. Styczek, The pressure problem in the stochastic vortex blob method, in *Vortex Flows and Related Numerical Methods II*, ESAIM: Proceedings (1996), Vol. 1, p. 101, http://www.emath.fr/proc/Vol.1/.

4. P. E. Saffman, *Vortex Dynamics*, Cambridge Monographs on Mechanics and Applied Mathematics (Cambridge Univ. Press, Cambridge, UK, 1992).

5. D. Shiels, A. Leonard, and A. Stagg, Computational investigation of drag reduction on a rotationally oscillating cylinder, in *Vortex Flows and Related Numerical Methods II*, ESAIM: Proceedings (1996), Vol. 1, p. 307, http://www.emath.fr/proc/Vol.1/.

6. F. Noca, D. Shiels, and D. Jeon, Measuring instantaneous fluid dynamic forces on bodies, using only velocity fields and their derivatives, *J. Fluids Struct.* **11**, 345 (1997).

7. F. Noca, *On the Evaluation of Time-Dependent Fluid-Dynamic Forces on Bluff Bodies*, Ph.D. thesis, (Cal Tech, 1997).

8. G. K. Batchelor, *An Introduction to Fluid Dynamics* (Cambridge Univ. Press, Cambridge, UK, 1967).

9. A. Styczek and P. Wald, Fast and efficient vortex blob simulation of the flow past the circular cylinder, *Arch. Mech. Eng.* **42**, 281 (1995).